Deprotonation of Carotenoid Radical Cation and Formation of a Didehydrodimer

Yunlong Gao, Sharon Webb, and Lowell D. Kispert*

Department of Chemistry, Box 870336, University of Alabama, Tuscaloosa, Alabama 35487-0336

Received: June 30, 2003; In Final Form: September 11, 2003

Deprotonation of the carotenoid radical cation ($Car^{\bullet+}$) in CH_2Cl_2 was studied by electrochemistry, optical, MALDI-TOF, and EPR spectroscopy. Water enhances deprotonation of the carotenoid radical cation. The formation of a didehydrodimer $(\#Car)_2$ (#Car: Car with one less proton) was confirmed by the above techniques. The structure of the dimer is proposed on the basis of semiempirical calculations, optical, and EPR studies.

Introduction

Carotenoids (Car) are widely distributed among plants, animals, and certain bacteria. They play a significant role in photosynthesis, because of their large absorption extinction coefficients, due to the long conjugated polyene chain they contain. In photosynthesis, carotenoids serve primarily as light-harvesting pigments and photoprotectors.[1,2] Several years ago formation and accumulation of the β-carotene radical cation in the photosystem II reaction center were detected. The process is induced by the photooxidized chlorophyll, $P680^{\bullet+}$ (Car donates an electron to $P680^{\bullet+}$).[3−5] $Car^{\bullet+}$ can also be formed by electron donation from Car to several oxy radicals, such as $CCl_3O_2^{\bullet}$, $RSO_2^{\bullet}$, $NO_2^{\bullet}$, and various aryl peroxyl radicals.[6]

Because $Car^{\bullet+}$ is involved in electron-transfer reactions in photosystem II and also in the process of scavenging oxy radicals by Car, the behavior of $Car^{\bullet+}$ needs to be studied to further understand its roles in the reactions. UV/vis absorption[7] and resonance Raman spectra[8] and isomerization,[9,10] of several carotenoid radical cations have been reported in some detail. The polarizability of the ground and excited states of carotenoid radical cations has also been evaluated.[11] A recent study[12] showed that $Car^{\bullet+}$ can react with O_2 to form 5,8-peroxides of Car. We report here some other aspects of the deprotonation of $Car^{\bullet+}$. CV[13−15] (cyclic votammetry) showed that during an electrochemical oxidation−reduction cycle in CH_2Cl_2, radical cations $Car^{\bullet+}$, dications Car^{2+}, cations $\#Car^{+}$ (loss of one H^+ from Car^{2+}), and neutral radicals $\#Car^{\bullet}$ (loss of one H^+ from $Car^{\bullet+}$) can be formed. Several electrode and homogeneous reactions (Scheme 1) have been identified.[9,16−21] The deprotonation of Car^{2+} (eq 5) was confirmed by simultaneous step voltammetry,[17] EPR,[17] OSWV,[16] and electrospray mass spectrometric studies.[22] However, little is known about the deprotonation product of $Car^{\bullet+}$. The proposed reaction (eq 6) is in agreement with electrochemical digital simulation of CV.[18−20]

In this study, electrochemistry, EPR, optical, and MALDI-TOF spectroscopies were used to examine the deprotonation of $Car^{\bullet+}$ of canthaxanthin (**I**) and β-carotene (**II**) (Chart 1). After the oxidation of Car by Fe^{3+} in CH_2Cl_2, a didehydrodimer $(\#Car)_2$ was detected by optical and MALDI-TOF techniques. Formation of the dimer is attributed to the coupling of $\#Car^{\bullet}$. Possible structures of $\#Car^{\bullet}$ and dimer $(\#Car)_2$, and the gas-phase maximum absorption wavelengths of the species $Car^{\bullet+}$, $\#Car^{\bullet}$, $(\#Car)_2$, and $(\#Car)_2^{\bullet+}$ were estimated by semiempirical calculations.

SCHEME 1

Electrode reactions:

$$Car \rightleftharpoons Car^{\bullet+} + e^- \quad (1)$$

$$Car^{\bullet+} \rightleftharpoons Car^{2+} + e^- \quad (2)$$

$$\#Car^{\bullet} \rightleftharpoons \#Car^{+} + e^- \quad (3)$$

Homogeneous reactions:

$$Car^{2+} + Car \rightleftharpoons 2Car^{\bullet+} \quad (4)$$

$$Car^{2+} \rightleftharpoons \#Car^{+} + H^+ \quad (5)$$

$$Car^{\bullet+} \rightleftharpoons \#Car^{\bullet} + H^+ \quad (6)$$

#Car represents the carotenoid with one less proton

CHART 1: Structures of I and II

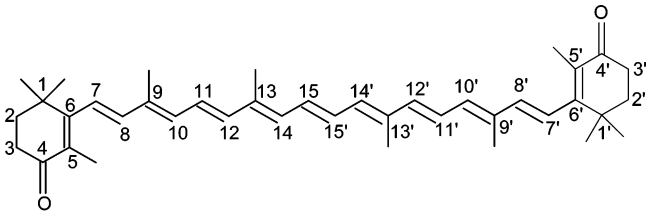

All-trans Canthaxanthin (**I**)

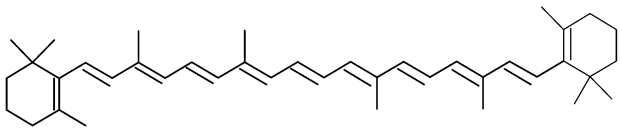

All-trans β-Carotene (**II**)

Experimental Section

Chemicals. Canthaxanthin (**I**), β-carotene (**II**), and the supporting electrolyte tetrabutylammonium hexafluorophosphate (TBAHFP) were purchased from Fluka. β-Carotene was purified by extraction with benzene and precipitation with methanol. Ferric chloride ($FeCl_3$) was purchased from Sigma. Anhydrous dichloromethane (CH_2Cl_2) was purchased from Aldrich. All CH_2Cl_2 solutions of carotenoids and $FeCl_3$ were prepared and sealed in a N_2 drybox before measurements.

Electrochemistry. CV (cyclic votammetry) measurements were performed with a BAS-100 B/W electrochemical analyzer in a conventional three-electrode system at room temperature.

10.1021/jp0358679 CCC: $25.00
Published on Web 11/01/2003

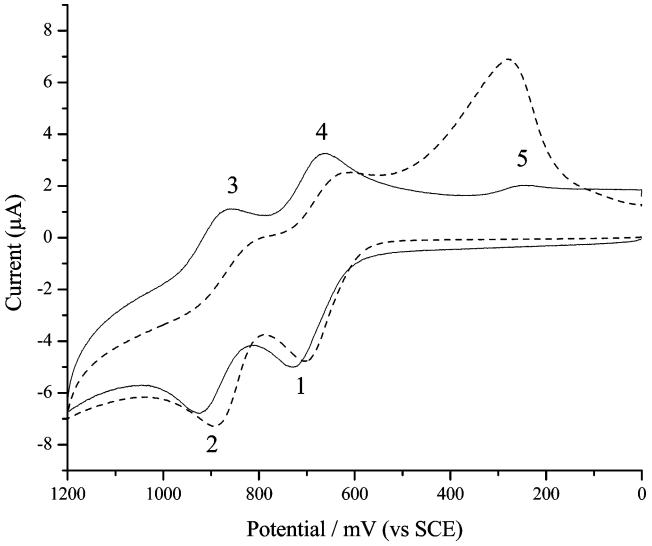

Figure 1. CV of **I** in CH_2Cl_2: solid line, that without water in the solution; dashed line, that with water in the solution.

A platinum disk electrode was selected as the working electrode, a platinum wire as the auxiliary electrode, and a saturated calomel electrode (SCE) as the reference electrode.

Optical Studies. Optical spectra were recorded with a double-beam Shimadzu UV−visible 1601 spectrophotometer (190−1100 nm) using 1 cm quartz cells.

MALDI-TOF MS. MALDI-TOF experiments were performed by using a Bruker Reflex III MALDI-TOF mass spectrometer with a nitrogen laser at 337 nm and a 2.9 m flight path with a gridless reflector. Indoleacrylic acid (Aldrich) was used as the matrix. Positive polarity, 100 laser shots, and the reflection mode were used in the experiment.

EPR. EPR measurements were carried out with an X-band (9.5 GHz) Varian (Palo Alto, CA) E-12 EPR spectrometer, equipped with a rectangular cavity. The magnetic field was measured with a Bruker (Billerica, MA) EPR 035M gaussmeter, and the microwave frequency was measured with a model HP 5245L frequency counter.

Semiempirical Calculations. AM1[23] and ZINDO/S[24] semiempirical molecular orbital calculations were carried out using Hyperchem 6.03 software on a Dell PC computer (Pentium III).

Results and Discussion

In the CV study of Car, we found that small amounts of water in the carotenoid CH_2Cl_2 solution enhance the deprotonation of $Car^{\bullet+}$ and Car^{2+}. Figure 1 shows the CV of **I** with and without water in the solution. Peaks 1 and 2 are oxidation peaks of Car and $Car^{\bullet+}$, respectively;[9,13−21] peaks 3−5 are reduction peaks of Car^{2+}, $Car^{\bullet+}$, and $\#Car^{+}$, respectively.[9,13−21] In the CV of the solution containing water, the reduction peaks 3 and 4 decrease and the reduction peak 5 increases significantly. Similar results were found for **II**. These phenomena can be explained by the fact that the equilibria are shifted to the right. The reactions are

$$Car^{\bullet+} \rightleftharpoons \#Car^{\bullet} + H^{+}$$

$$Car^{2+} \rightleftharpoons \#Car^{+} + H^{+}$$

$$H^{+} + H_2O \rightleftharpoons H_3{}^{+}O$$

The deprotonation product of $Car^{\bullet+}$ is the neutral radical $\#Car^{\bullet}$ and its reduction peak is not detected in the CV measurements.

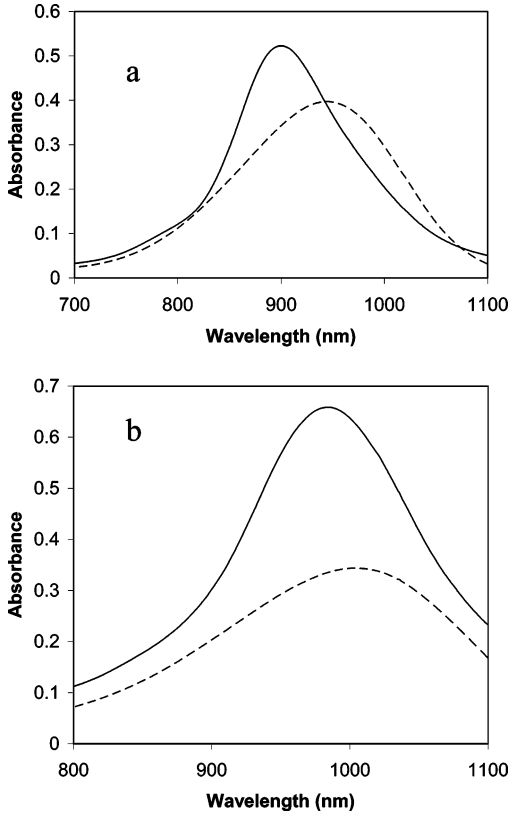

Figure 2. UV/vis spectra of $Car^{\bullet+}$ of **I** (a) and **II** (b) upon the addition of water (5 mM) to the reaction mixture of 10 μM of $FeCl_3$ and 100 μM of Car. Key: solid line, before adding water; dashed line, after adding water.

To observe the deprotonation of $Car^{\bullet+}$, UV/vis/NIR spectroscopy was used. Oxidation of Car by $FeCl_3$ in CH_2Cl_2 is known to produce stable $Car^{\bullet+}$,[7,11,12,25] which is observable in the NIR region. The equilium[12] reaction is

$$Car + Fe^{3+} \rightleftharpoons Car^{\bullet+} + Fe^{2+}$$

In this study, the concentrations of Car and Fe^{3+} are 100 and 10 μM, respectively. The solid lines in Figure 2a,b show the absorption spectra of $Car^{\bullet+}$ (**I**) and $Car^{\bullet+}$ (**II**), respectively, and are due to the $D_0 \rightarrow D_2$ transition.[7] Only a slight decrease in intensity occurred during the next 60 min in the absence of water and O_2. In the presence of water (~5 mM), the absorbance of $Car^{\bullet+}$ decreases significantly and a new red-shifted absorption peak (Figure 2a,b) appears. The new absorption peak may be due to the deprotonation product ($\#Car^{\bullet}$) of $Car^{\bullet+}$. ZINDO/S[24] calculations are useful for predicting UV/vis spectra. A previous study[7] showed that, although the absolute values of the calculated absorption wavelengths do not match the experimental values, the relative absorption wavelengths for different species of carotenoid and the relative oscillator strengths show the same trend as the experimental values. To perform ZINDO/S calculations of ($\#Car^{\bullet}$) and $Car^{\bullet+}$, the structures of these species should be established. For $\#Car^{\bullet}$, the proton loss site should be known. According to previous studies,[17−20] the proton loss site should be from a methyl group at positions 5/5′, 9/9′, or 13/13′. Proton loss from the CH groups of the polyene chain is unlikely, because the product radical cannot be stabilized by resonance. The EPR study[17] of the reduction product of $\#Car^{+}$ showed that $\#Car^{\bullet}$ has an EPR spectrum with a line width of about 13 G, typical for a delocalized radical. If a proton were lost from a CH group in the polyene chain, the resulting vinyl-type radical

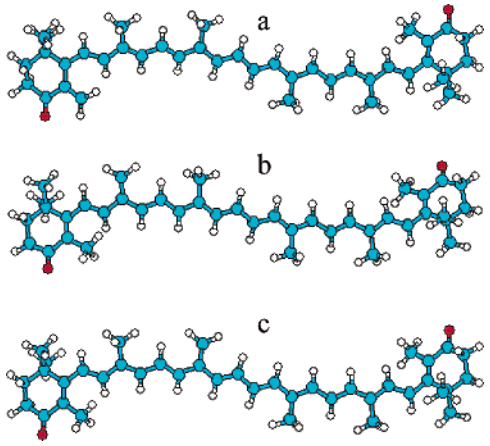

Figure 3. Optimized geometries of #Car•(5) (a), #Car•(9) (b), and #Car•(13) (c) of **I**.

TABLE 1: Total Energy (kcal/mol) of #Car• Calculated by AM1-UHF

Car	#Car•(5)	#Car•(9)	#Car•(13)
I	−149037.9	−149035.3	−149034.8
II	−135552.7	−135548.7	−135548.6

TABLE 2: Maximum Absorption Wavelength (nm) of Carotenoid Species Calculated by ZINDO/S

Car	Car•+	#Car•(5)	#Car•(9)	#Car•(13)
I	858	562	492	440
II	872	549	504	438

should give rise to two EPR lines separated by 82 G. Geometry optimizations of #Car•(5) (proton loss at 5 methyl), #Car•(9) (proton loss at 9 methyl), and #Car•(13) (proton loss at 13 methyl) are by AM1-UHF. The X-ray structures[26] of **I** and **II** were used as inputs to perform the calculations. The optimized structures of #Car•(5), #Car•(9), and #Car•(13) of **I** are shown in Figure 3. For #Car•(5), the minimum energy is obtained when the torsion angle of C7−C6−C5−C(5 methyl) is 20.3°; for #Car•(9) and #Car•(13), the minimum energy of #Car• is obtained when the plane of CH_2• formed by the two C−H bonds is coplanar with the chain. Similar results are obtained for **II**. Table 1 shows the total energy (kcal/mol) of #Car• calculated by AM1-UHF. The calculations show that the energy of #Car•(5) is slightly lower than those of #Car•(9) and #Car•(13). Whether this is attributable to retention of the π-system when a proton is removed from the 5 methyl rather than from 9 or 13 methyl or this is in the calculation error range is unclear. We tentatively assume that proton losses from the three sites are equally probable, although Jeevarajan[20] suggested that proton loss at 5/5′ methyl is less likely because the cyclohexene double bonds are not coplanar with the chain and thus poor overlap of 5/5′ CH_2• occurs with the π-system. These gas-phase geometries were used for a single-point ZINDO/S calculation. The single-excitation configuration interaction involving about 100 configurations was used to calculate the optical absorption spectrum. The weighting factors for $\sigma-\sigma$ and $\pi-\pi$ overlap are 1.267 and 0.585, respectively. The results (Table 2) indicate that the absorption peak of #Car• should be blue-shifted compared to that of Car•+. However, no such absorption was observed in the reaction solution, indicating that #Car• (if it is produced) is either not stable or very reactive (other product may be formed from the radical). The new absorption peak that is red-shifted compared to that of Car•+ must be due to another product.

MALDI-TOF MS in the positive mode was used to detect the products after water had been added to the reaction solution.

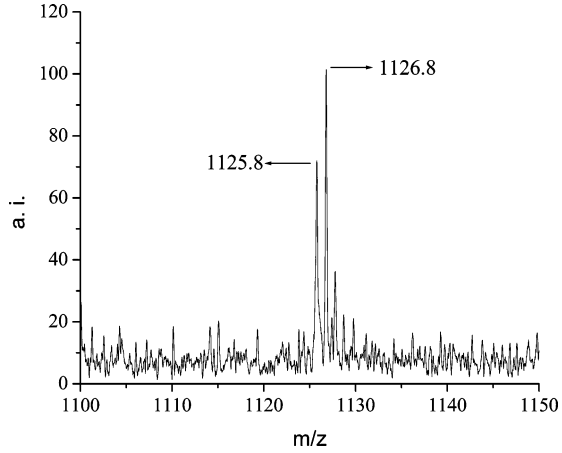

Figure 4. MALDI-TOF mass spectrum of $(\#Car)_2^{\bullet+}$ and $\#(\#Car)_2^{+}$ of **I**.

The molecular ion of the dimer $(\#Car)_2$ and $[(\#Car)_2-H]^{\bullet}$ were detected (formation of $[(\#Car)_2-H]^{+}$ is probably a result of laser irradiation in the MALDI-TOF experiment). As expected, these species were not detected when water was not added, indicating the formation of the dimers is due to water. The mass spectra of $(\#Car)_2$ and $[(\#Car)_2-H]^{\bullet}$ of **I** are shown in Figure 4. The molecular mass of the dimer of **I** is 1126.8 (calculated using the mass of isotopes with the greatest abundance).

Geometry optimization of various dimers was performed by AM1-UHF. Because these dimers are large molecules, locating the global minimum energy of these dimers is very difficult. In an effort to address this difficulty, energies of dozens of structures were calculated and compared. The geometry-optimized monomers shown in Figure 3 were used as inputs to perform the calculation. A bond was built between the two monomers at the 5 or 9 or 13 methyl proton loss position of each monomer and then the geometry optimization was performed. Many initial relative orientations of the monomer chain were examined, and the optimized dimer structure was found to depend on the relative initial orientation of the two monomers. The calculations show that the dimer with the least repulsive force between the two monomers (and thus the least disruption of the π-system of the monomer) is the most stable. Figure 5 shows the most stable structures we calculated so far for dimers (**I**) $(\#Car)_2(5-5)$ (dimer formed by two #Car•(5)), $(\#Car)_2(9-9)$ (dimer formed by two #Car•(9)), and $(\#Car)_2(13-13)$ (dimer formed by two #Car•(13)). Similar structures were obtained for $(\#Car)_2$ (**II**). Table 3 shows the total energy (kcal/mol) of $(\#Car)_2$ calculated by AM1-UHF. $(\#Car)_2(5-5)$ formed by connecting the two monomers end to end (shown in Figure 5) is the most stable structure by a considerable margin because this structure causes the least structure change of the monomers. The optimized structures of $(\#Car)_2(9-9)$ and $(\#Car)_2(13-13)$ cause significant disruption of the conjugated π-system in the monomers, and thus the structures are less stable than that of $(\#Car)_2(5-5)$. $(\#Car)_2(9-9)$ is less stable than $(\#Car)_2(5-5)$ by 140.5 and 94.9 kcal/mol for **I** and **II**, respectively. $(\#Car)_2(13-13)$ is less stable than $(\#Car)_2(9-9)$ by 53.5 and 42.4 kcal/mol for **I** and **II**, respectively. The calculated enthalpy for the dimer formation reaction is in the range −100 to −300 kcal/mol depending on the structure of the dimer, indicating that dimer formation is favorable at room temperature. ZINDO/S calculations of the dimers were also performed to determine whether the absorption of $(\#Car)_2$ or of $(\#Car)_2^{\bullet+}$ is expected to be red-shifted compared to that of Car•+. The formation of $(\#Car)_2^{\bullet+}$ can be due to the following:

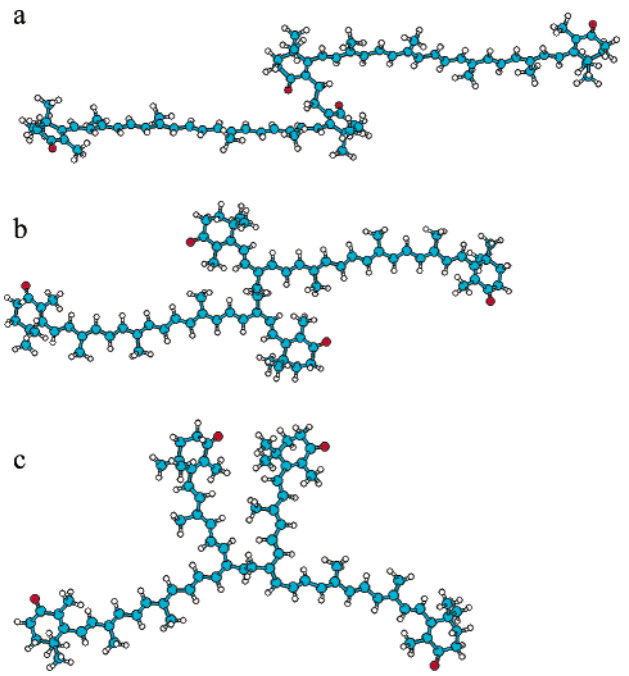

Figure 5. Optimized geometries of $(\#Car)_2(5-5)$ (a), $(\#Car)_2(9-9)$ (b), and $(\#Car)_2(13-13)$ (c) of **I**.

TABLE 3: Total Energy (kcal/mol) of $(\#Car)_2$ Calculated by AM1-UHF

Car	$(\#Car)_2(5-5)$	$(\#Car)_2(9-9)$	$(\#Car)_2(13-13)$
I	−298506.4	−298365.9	−298312.4
II	−271199.9	−271105.0	−271062.6

TABLE 4: Maximum Absorption Wavelength (nm) of Carotenoid Species Calculated by ZINDO/S

		dimer (5−5)		dimer (9−9)		dimer (13−13)	
Car	$Car^{\bullet+}$	$(\#Car)_2$	$(\#Car)_2^{\bullet+}$	$(\#Car)_2$	$(\#Car)_2^{\bullet+}$	$(\#Car)_2$	$(\#Car)_2^{\bullet+}$
I	858	612	1290	662	723	528	613
II	872	572	1286	389	781	396	524

$$(\#Car)_2 + Fe^{3+} \rightleftharpoons (\#Car)_2^{\bullet+} + Fe^{2+}$$

$$(\#Car)_2 + Car^{\bullet+} \rightleftharpoons (\#Car)_2^{\bullet+} + Car$$

The calculated gas phase absorption wavelengths listed in Table 4 show that only the absorption maximum of $(\#Car)_2^{\bullet+}(5-5)$ is red-shifted, implying that only $(\#Car)_2^{\bullet+}(5-5)$ is formed. The explanation is that either proton loss from $Car^{\bullet+}$ occurs only from the 5/5′ methyl group or only two $\#Car^{\bullet}(5)$ can form a dimer because $(\#Car)_2(5-5)$ is the most stable. The fact that the new absorption peak is not due to neutral $(\#Car)_2$ was confirmed by EPR spectroscopy.

Conclusions

This study presents evidence that in the chemical oxidation of Car, a didehydrodimer $(\#Car)_2$ [probably $(\#Car)_2(5-5)$] can be formed from $\#Car^{\bullet}$, which in turn is the deprotonation product of $Car^{\bullet+}$. The deprotonation is enhanced by water. The absorption peak of $(\#Car)_2^{\bullet+}$ is red-shifted compared to that of the symmetrical $Car^{\bullet+}$. These results should be useful in the assignment of optical absorption spectra of other carotenoid products.

Acknowledgment. We thank Dr. E. Hand for helpful discussions. This work was supported by the Division of Chemical Sciences, Office of Basic Energy Sciences, Office of Energy Research, of the U.S. Department of Energy under Grant No. DE-FG02-86ER13465.

References and Notes

(1) Koyama, Y. *J. Photochem. Photobiol. B* **1991**, *9*, 265.

(2) Koyama, Y.; Kuki, M.; Andersson, P. O.; Gillbro, T. *Photochem. Photobiol.* **1996**, *63*, 243.

(3) Schenck, C. C.; Diner, B.; Mathis, P.; Satoh, K. *Biochim. Biophys. Acta* **1982**, *680*, 216.

(4) Mathis, P.; Rutherford, A. *Biochim. Biophys. Acta* **1984**, *767*, 217.

(5) De Las Rivas, J. O.; Telfer, A.; Barber, J. *Biochim. Biophys. Acta* **1993**, *1142*, 155.

(6) Edge, R.; Truscott, T. G. In *The Photochemistry of Carotenoids*; Frank, H. A., Young, A. J., Britton, G., Cogdell, R. J., Eds.; Kluwer: The Netherlands, 1999; pp 223−234.

(7) Jeevarajan, J. A.; Wei, C.-C.; Jeevarajan, A. S.; Kispert, L. D. *J. Phys. Chem.* **1996**, *100*, 5637.

(8) Jeevarajan, A. S.; Kispert, L. D.; Chumanov, G.; Zhou, C.; Cotton, T. M. *Chem. Phys. Lett.* **1996**, *259*, 515.

(9) Wei, C.-C. Ph.D. Dissertation, University of Alabama, Tuscaloosa, 1996.

(10) Gao, G.; Wei, C.-C.; Jeevarajan, A. S.; Kispert, L. D. *J. Phys. Chem.* **1996**, *100*, 5362.

(11) Krawczyk, S. *Chem. Phys.* **1998**, *230*, 297.

(12) Gao, Y.; Kispert, L. D. Submitted to *J. Phys. Chem. B.*

(13) Mairanovsky, V. G.; Engovatov, A. A.; Ioffe, N. T.; Samokhvalov, G. I. *J. Electroanal. Chem.* **1975**, *66*, 123.

(14) Khaled, M.; Hadjipetrou, A.; Kispert, L. D. *J. Phys. Chem.* **1991**, *95*, 2438.

(15) Jeevarajan, A. S.; Khaled, M.; Kispert, L. D. *J. Phys. Chem.* **1994**, *98*, 7777.

(16) Chen, X., M. S. Thesis, University of Alabama, Tuscaloosa, 1991.

(17) Khaled, M., Ph.D. Dissertation, University of Alabama, Tuscaloosa, 1992.

(18) Jeevarajan, J. A.; Kispert, L. D. *J. Electroanal. Chem.* **1996**, *411*, 57.

(19) Jeevarajan, J. A.; Jeevarajan, A. S.; Kispert, L. D. *J. Chem. Soc., Faraday Trans.* **1996**, *92*, 1757.

(20) Jeevarajan, J. A. Ph.D. Dissertation, University of Alabama, Tuscaloosa, 1995.

(21) Liu, D.; Gao, Y.; Kispert, L. D. *J. Electroanal. Chem.* **2000**, *488*, 140.

(22) Van Berkel, G. J.; Zhou, F. *Anal. Chem.* **1994**, *66*, 3408.

(23) Dewar, M. J. S.; Zoebisch, E. E.; Healy, E. F.; Stewart, J. J. P. *J. Am. Chem. Soc.* **1985**, *107*, 3902.

(24) (a) Ridley, J.; Zerner, M. C. *Theor. Chim. Acta* **1973**, *32*, 111. (b) Ridley, J.; Zerner, M. C. *Theor. Chim. Acta* **1976**, *42*, 223.

(25) Wei, C.-C.; Gao, G.; Kispert, L. D. *J. Chem. Soc., Perkin Trans.* **1997**, *2*, 783.

(26) Hashimoto, H.; Yoda, T.; Kobayashi, T.; Young, A. J. *J. Mol. Struct.* **2002**, *604*, 125.